On-chip methane sensing by near-IR absorption signatures in a photonic crystal slot waveguide

Wei-Cheng Lai,[1] Swapnajit Chakravarty,[2,*] Xiaolong Wang,[2] Cheyun Lin,[1] and Ray T. Chen[1]

[1]*Department of Electrical and Computer Engineering, University of Texas at Austin, Austin, Texas 78712, USA*

[2]*Omega Optics, Inc., 10306 Sausalito Drive, Austin, Texas 78759, USA*

**Corresponding author: swapnajit.chakravarty@omegaoptics.com*

Received December 21, 2010; revised February 12, 2011; accepted February 17, 2011;
posted February 18, 2011 (Doc. ID 139906); published March 14, 2011

We demonstrate a 300 μm long silicon photonic crystal (PC) slot waveguide device for on-chip near-infrared absorption spectroscopy, based on the Beer–Lambert law for the detection of methane gas. The device combines slow light in a PC waveguide with high electric field intensity in a low-index 90 nm wide slot, which effectively increases the optical absorption path length. A methane concentration of 100 ppm (parts per million) in nitrogen was measured.

OCIS codes: 280.4788, 300.6340, 230.5298.

Infrared (IR) absorption spectroscopy is widely used as a simple and reliable technique for detection and identification of hazardous and greenhouse gases in the atmosphere. IR spectroscopy relies on fundamental molecular vibrations, which makes the technique very attractive for sensing and identification when compared to other methods. Various methods, such as cavity ring-down spectroscopy (CRDS) [1,2], tunable diode laser absorption spectroscopy (TDLAS) [3], and Fourier transform IR spectroscopy [4] that detect gases through spectroscopic signatures, are available commercially. Except for a handheld TDLAS methane sensor [5], most commercial IR spectrometers are large, heavy tabletop instruments consuming a few tens to hundreds of watts of power. The above characteristics make the instruments expensive and unsuitable for portable distributed sensing applications. A lab-on-chip IR absorption spectrometer for gases is thus highly desirable.

The principle of IR absorption spectroscopy is based on the Beer–Lambert law. According to this law, the transmitted intensity I is given by

$$I = I_0 \times \exp(-\gamma \alpha L), \tag{1}$$

where I_0 is the incident light intensity, α is the absorption coefficient of the analyte medium, L is the optical interaction length, and γ is the medium-specific absorption factor that is determined by the dispersion-enhanced light–matter interaction. In conventional free-space systems, $\gamma = 1$; hence, L must be large to achieve a suitable sensitivity of measured I/I_0. For lab-on-chip systems, L must be small; hence, γ must be large. Using the perturbation theory [6], it can be shown that

$$\gamma = f \times \frac{c/n}{v_g}, \tag{2}$$

where c is the velocity of light, v_g is the group velocity in the analyte of the effective index n, and f is the fill factor, which denotes the relative fraction of the optical field that resides in the analyte. Equation (2) shows that slow light propagation (small v_g) significantly enhances absorption. Furthermore, the greater the electric field overlap with the analyte, the greater the effective absorption by the medium. Both features of small v_g and high f are satisfied in a photonic crystal (PC) slot waveguide. PC devices have unique dispersive properties that allow control and manipulation of light–matter interactions on length scales of the wavelength of light [7,8]. PC devices have been demonstrated for light emission [9], sensing [10], and electro-optical modulation [11] among various applications.

PC waveguides have demonstrated group velocity slowdown factors of ~100 [12]. Slot waveguides have also demonstrated a significant increase in the electric field intensity in a narrow low-index slot in a high-index ridge waveguide, by at least a factor of 10 [13]. Slow light in PC waveguides coupled with electric field intensity enhancement in a slot in the PC waveguide can thus reduce v_g and enhance f, thereby theoretically shrinking the absorption path length by a factor of 1000, an order of magnitude greater than ring resonator devices [14]. We previously demonstrated near-IR spectroscopy of xylene in a water ambient [15] with a PC slot waveguide. Here, we demonstrate a PC slot waveguide for on-chip near-IR absorption spectroscopy of methane, a typical greenhouse gas.

The schematic of our silicon PC slot waveguide device is shown in Fig. 1(a). The PC waveguide is a W1.3 line defect with a uniform lattice constant a and width of $1.3 \times \sqrt{3}a$. The device parameters are shown in Fig. 1(a). The dispersion relation of the defect-guided mode is calculated using the three-dimensional plane-wave expansion method in Fig. 1(b). In contrast to a fragile freestanding silicon platform, we choose a silicon-on-insulator (SOI) platform that provides more mechanical stability. Three modes labeled 1, 2, and 3 are observed in the photonic bandgap. Mode profiles are shown in the insets to Fig. 1(b). Modes 1 and 3 are slot guided modes. However, only mode 3 propagates below the light line for silicon dioxide, without any overlap with modes above the light line. Mode 2 resides primarily in the dielectric and air holes; hence, it interacts less with the analyte filling the slot. The design parameters of the W1.3 PC slot waveguide are thus chosen corresponding to mode 3. Light is guided in and out of the PC slot waveguide by ridge waveguides using a PC impedance taper for higher coupling efficiency into the slow light mode, where holes

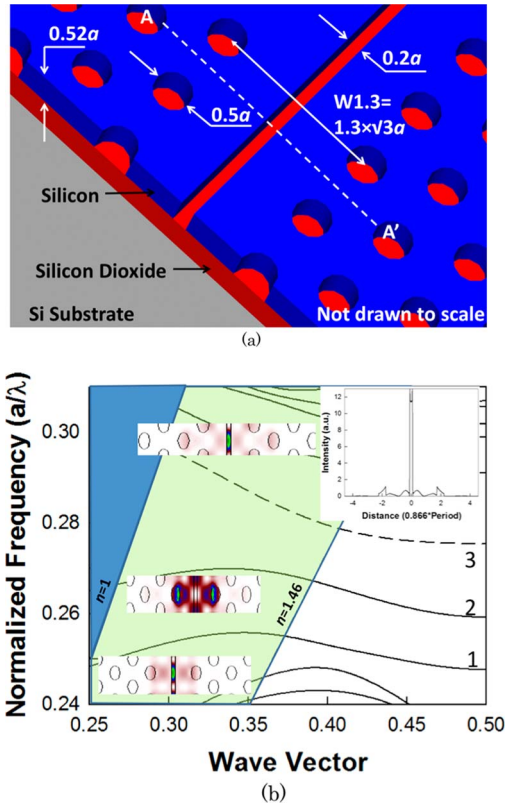

Fig. 1. (Color online) (a) Schematic of the PC slot waveguide device showing different regions: a denotes the lattice constant. (b) Dispersion diagram of PC slot waveguide showing different modes. Insets, mode profiles of modes 1, 2, and 3 across axis A–A' in (a). Electric field enhancement magnitude as a function of position for mode 3 across axis A–A' is shown.

adjacent to the PC slot waveguide are shifted in steps by $0.00125 \times \sqrt{3}a$ over 16 periods [16].

Device fabrication on the SOI wafer follows standard steps described in detail elsewhere [13,16,17]. A scanning electron micrograph (SEM) of the fabricated structure is shown in Fig. 2. While electric field enhancement by the slot is nearly constant across the entire bandwidth of the guided mode, as observed in the group index simulation in Fig. 3, slow light effects decrease rapidly from the band edge, reaching $n_g = 30$ about 5 nm from the band edge.

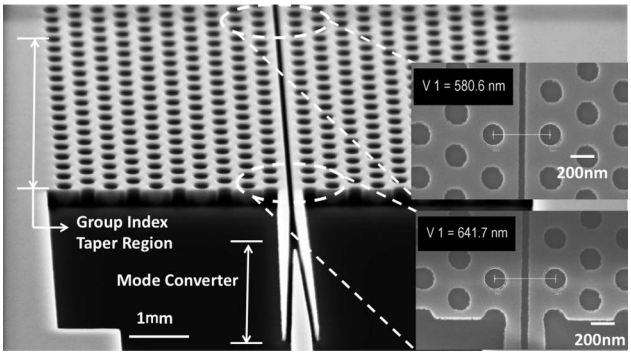

Fig. 2. SEM image of fabricated W1.3 PC slot waveguide device, showing input mode converter, input group index taper, and etched PC pattern. Insets, distance between air holes on two sides of the slot at the beginning and the end of the group index taper.

To derive maximum absorbance enhancement, it is necessary to ensure that the slow light effects are maximum at the absorbance peak. A theoretical absorbance spectrum of methane in near-IR shows that a broad signature exists between 1665 and 1668 nm, with the peak at 1665.5 nm [17]. It is important to consider propagation losses that occur at low group velocities. Design parameters are chosen so that the group index n_g of the guided mode is ~40 at 1665.5 nm; correspondingly, the band edge occurs at ~1668.5 nm. Input light from a broadband source was TE polarized and butt coupled to/from the device with a polarization-maintaining single-mode tapered lensed fiber with mode field diameter of ~3 μm.

The experimental transmission spectrum in Fig. 3 shows that the band edge is redshifted ~1.5 nm from the design to 1670 nm. A mixture of 4% methane (CH_4) in nitrogen (N_2) from Matheson Tri-Gas, was diluted to various concentrations in N_2 using factory-calibrated rotameter settings at 20 psi pressure. The transmitted light was analyzed with an Ando AQ6317B optical spectrum analyzer with a noise floor of –95 dBm, in the presence and absence of CH_4 at normal temperature and pressure (NTP). The absorbance of CH_4 is calculated as $\Delta A = A_a - A_{am} = \log_{10}(P_a/P_{am})$, where P_{am} and A_{am} denote transmitted power and absorbance, respectively, in the presence of CH_4, while P_a and A_a denote transmitted power and absorbance, respectively, in the absence of CH_4, in N_2 ambient.

Response time is determined by the signal integration time of 45 s. Measurements are performed immediately after gas introduction. The theoretical spectrum of CH_4 [17] is shown in Fig. 4 as a black scatterplot with a peak at 1665.5 nm. The experimentally obtained CH_4 absorbance spectrum is shown for different concentrations. A peak is observed at 1665.5 nm with a broad shoulder around 1667.5 nm. Spectra are calculated from experimental transmission spectra for several CH_4 mixing ratios. The absorbance magnitude at 1665.5 nm versus concentration is plotted in the inset of Fig. 4.

As seen in simulations in Fig. 3, the group index varies rapidly; near the band edge, the group index is greater than 100, while ~5 nm away from the band edge, the group index drops to ~30. A higher group index close to the band edge leads to unequal absorbance enhancements; hence, a broad shoulder is observed in

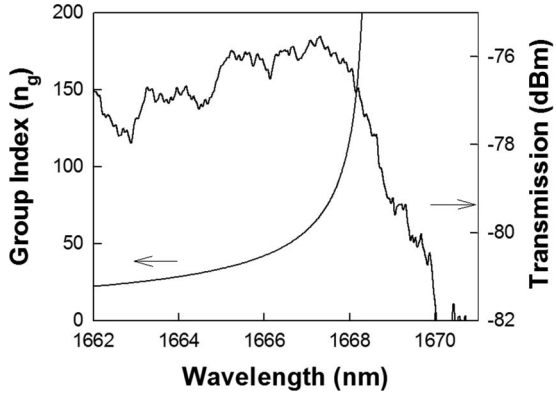

Fig. 3. (left axis) Group index versus wavelength as designed in simulations with the band edge at ~1668.5 nm. (right axis) Experimental transmission spectrum (without analyte), showing the band edge shifted in fabricated device to 1670 nm.

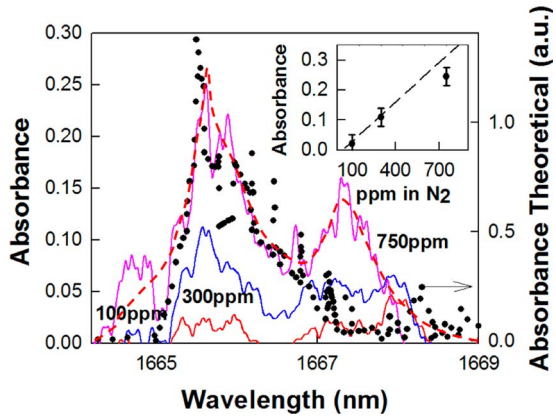

Fig. 4. (Color online) (right axis) The theoretical absorbance spectrum of methane obtained from [17] is shown by the dotted scatterplot. (left axis) Experimental absorbance of methane at various concentrations. The red dashed curve is a smoothed trace of the spectrum at 750 ppm. Inset, peak absorbance magnitude at 1665.5 nm versus concentration.

the experimental absorbance at 1667.5 nm. Gas concentrations down to 100 ppm [0.2% permissible exposure limit (PEL)] were measured, lower than requirements set by the Occupational Safety and Health Administration, at 500 ppm (or 1% PEL).

The sensitivity of the device is thus a strong function of the position of the band edge and hence fabrication imperfections. The number density of molecules per unit volume that can be determined by absorption spectroscopy [18] is given by

$$N_{\min} = \left(\frac{dI}{I_0}\right)/S(\nu)L, \tag{3}$$

where dI/I_0 is the fractional change in light intensity that can be detected, L is the effective absorption path length, and $S(\nu)$ is the absorption cross section of CH_4 at $1.665\,\mu\text{m} = 1.6 \times 10^{-20}\,\text{cm}^2$ [17]. In our measurements, $dI/I_0 \sim 5 \times 10^{-4}$. From Fig. 1(b), the slot electric field enhancement factor is ~12; if $n_g = 100$, the expected detection sensitivity from Eq. (3) by dividing the number density by the number of molecules per unit volume at NTP is ~40 ppm. By comparing the transmission spectrum with simulations, it is estimated that at 1665.5 nm, $n_g \sim 30$ experimentally. Hence less sensitivity is achieved in the experiment. By better control of fabrication, the band edge can be shifted closer to the absorbance peak. Because the waveguide loss is proportional to the group index squared, we believe that detection sensitivity for methane in near-IR can be increased by at least a factor of 2 with our 300 μm long device.

To our knowledge, our device is the only on-chip device demonstrated for IR absorption spectroscopy of gases; other devices sense refractive index changes only [19,20]. A complete lab-on-chip spectrometer can be made by integrating our device with an on-chip tunable laser and detector. When compared to commercial off-chip handheld TDLAS systems with near-IR sensitivity 1 ppm-m [5] or benchtop TDLAS systems with sensitivity of 0.1 ppm-m, our device has a near-IR sensitivity 0.03 ppm-m (100 ppm × 300 μm), consuming less than 20 mW power. When combined with wavelength/frequency modulation [21] in the near-IR, further enhancement in sensitivity by more than an order of magnitude is expected. The PC slot waveguide device, based on Maxwell's equations, is also readily scalable to the mid-IR. Because methane has an ~2 orders larger absorption cross section at 3.3 μm [17], high parts per billion (ppb) detection sensitivity can be achieved in PC slot waveguide devices on 300 μm length scales in the mid-IR with direct absorption spectroscopy, with low ppb sensitivities achieved when combined with wavelength/frequency modulation. Such low sensitivities can potentially be achieved without the need for high reflectivity mirrors and 200 watts of power in CRDS [1,2]. Multiple PC waveguides can be fabricated, each with a different period, to measure absorbance in the corresponding wavelength range, and identify gases in a mixture uniquely by comparing them with known IR absorbance databases.

In summary, we detected 100 ppm methane on-chip by near-IR absorption signatures, with a 300 μm long silicon PC slot waveguide. Remote monitoring is enabled by optical fibers.

The authors acknowledge the Environmental Protection Agency for funding this work under the Small Business Innovation Research program (grant EP-D-10-047).

References

1. M. J. Thorpe, K. D. Moll, R. J. Jones, B. Safdi, and J. Ye, Science **311**, 1595 (2006).
2. http://www.tigeroptics.com/.
3. M. Lackner, Rev. Chem. Eng. **23**, 65 (2007).
4. F. Adler, P. Maslowski, A. Foltynowicz, K. C. Cossel, T. C. Briles, I. Hartl, and J. Ye, Opt. Express **18**, 21861 (2010).
5. http://www.tdlas.com/products/.
6. N. A. Mortensen and S. S. Xiao, Appl. Phys. Lett. **90**, 141108 (2007).
7. E. Yablonovitch, Phys. Rev. Lett. **58**, 2059 (1987).
8. S. John, Phys. Rev. Lett. **58**, 2486 (1987).
9. S. Chakravarty, P. Bhattacharya, and Z. Mi, IEEE Photon. Technol. Lett. **18**, 2665 (2006).
10. S. Chakravarty, J. Topoľančik, P. Bhattacharya, S. Chakrabarti, Y. Kang, and M. E. Meyerhoff, Opt. Lett. **30**, 2578 (2005).
11. C.-Y. Lin, X. Wang, S. Chakravarty, B.-S. Lee, W.-C. Lai, J. Luo, A. K.-Y. Jen, and R. T. Chen, Appl. Phys. Lett. **97**, 093304 (2010).
12. M. Notomi, Phys. Rev. Lett. **87**, 253902 (2001).
13. X. Chen, W. Jiang, J. Chen, L. Gu, and R. T. Chen, Appl. Phys. Lett. **91**, 091111 (2007).
14. A. Nitkowski, L. Chen, and M. Lipson, Opt. Express **16**, 11930 (2008).
15. W.-C. Lai, S. Chakravarty, X. Wang, C. Lin, and R. T. Chen, Appl. Phys. Lett. **98**, 023304 (2011).
16. X. Wang, S. Chakravarty, B.-S. Lee, C. Lin, and R. T. Chen, Opt. Lett. **34**, 3202 (2009).
17. http://www.cfa.harvard.edu/HITRAN/.
18. W.-B. Yan, Gases Technol. **1** (4), 21 (2002).
19. J. T. Robinson, L. Chen, and M. Lipson, Opt. Express **16**, 4296 (2008).
20. N. A. Yebo, P. Lommens, Z. Hens, and R. Baets, Opt. Express **18**, 11859 (2010).
21. A. Karpf and G. N. Rao, Appl. Opt. **49**, 1406 (2010).